Available online at www.sciencedirect.com
ScienceDirect
Solar Energy 83 (2009) 1360–1369
SOLAR ENERGY
www.elsevier.com/locate/solener

Design and experimental performance of a PV Ice-maker without battery

Petros J. Axaopoulos *, Michael P. Theodoridis

Department of Energy Technology, Technological Educational Institute of Athens, Agiou Spyridona street, 12210 Egaleo, Athens, Greece

Received 28 November 2007; received in revised form 4 November 2008; accepted 2 March 2009
Available online 31 March 2009

Communicated by: Associate Editor Elias Stefanakos

Abstract

This paper presents a solar photovoltaic powered ice-maker which operates without the use of batteries and is therefore environmentally friendly and may be used in truly autonomous applications in remote areas. The successful operation of the refrigeration compressors by the PV panels is ensured by the use of a novel concept dedicated controller, which provides easy startup, maximum power tracking and power management for the four compressors of the system. The prototype results have shown very good ice-making capability and reliable operation as well as a great improvement in the startup characteristics of the compressors, which remain operational even during days with low solar irradiation and operate with improved utilization of the available photovoltaic power.

Keywords: Autonomous PV system; Ice-maker; Solar freezer; Variable speed compressor; Batteryless

1. Introduction

Among the various and interesting applications of solar energy, the production of ice can be considered as an important social and economic benefit to remote areas and developing countries since it can be used for the preservation of agricultural products, food, medicines and vaccines. At present, the most common technologies to produce ice, using solar energy, are heat driven ice maker, with numerous investigations (Boubakri, 2006; Buchter et al., 2003; Hildbrand et al., 2004; Khattab, 2006; Leite and Daguenet, 2000; Li et al., 2004; Luo et al., 2005; Wang et al., 2000) and electrically driven ice maker, where the electricity is produced by photovoltaic panels and the ice is formed mainly on freezer which is an integral part of the refrigerator. Although many studies have been performed in this latter technology, most of them are based on the vapor compression cycle where the compressor is driven by photovoltaic through a battery, charge controller (El Tom et al., 1991; Taha, 1995; Toure and Fassinou, 1999; Kaplanis and Papanastasiou, 2006) and inverter (Kattakayam and Srinivasan, 1998, 2000).

In order to eliminate the battery, charge controller and inverter with their associated environmental, operating and economic problems, a solar photovoltaic ice-making system, without battery, charge controller and inverter has been developed in the Renewable Energy Laboratory at the Technological Educational Institute of Athens. Our approach is to store the energy in ice and therefore to avoid the need for batteries, which are responsible for a significant portion of the capital cost and much of the maintenance cost. Additionally environmental pollution might be expected from batteries, due to their contaminating elements and because their life cycle is limited. Deep cycle batteries do not last more than about 1500 charge/discharge cycles and are usually not produced in developing countries, making funding, purchasing and transporting them to remote sights difficult. In addition, funds

* Corresponding author. Tel.: +00302105385396; fax: +00302105385306.
E-mail address: pax@teiath.gr (P.J. Axaopoulos).

0038-092X/$ - see front matter © 2009 Elsevier Ltd. All rights reserved.
doi:10.1016/j.solener.2009.03.007

may not be available to pay for the batteries when replacement is necessary. Recycling the used batteries is also very difficult and usually is rare. Generally, batteries in photovoltaic applications often present many problems (Diaz and Lorenzo, 2001; Spiers and Rasinkoski, 1996), most of them are related to their operating conditions as inability of the battery to get fully charged in such applications (Wagner and Sauer, 2001; Stevens et al., 1993; Woodworth et al., 1994).

The new trend in solar operated or assisted thermal systems is to incorporate the use of a direct-current, variable speed compressor. It has been shown in several research works that there occur reasons why compressors with capacity control offer distinct advantages over compressors with fixed capacity, especially concerning energy management and overall system efficiency (Bessler and Hwang, 1980; Chatuverdi and Abazeri, 1987; Chatuverdi et al., 1998; Hawlader et al., 2001; Kuang et al., 2003; Li et al., 2007).

In our system, the PV panel is connected directly to a capacity-modulated DC compressor via an efficient controller developed in our Laboratory. The advantage of using the developed controller is the improved utilization of the PV electric energy, achieved by modifying the compressor startup characteristics and exploiting the maximum power of the PV. In addition, the capacity modulation enables continuous efficient operation and also avoids the energy and mechanical costs of repeated start–stop cycles. A commercially available compressor is connected with a coolant circuit which is in thermal contact with the evaporator in the ice storage tank interior.

The ice storage tank consists of an inoxydable insulated water tank with a submerged evaporator. The advantage of having an ice storage tank is the small required stores, 14–21% of the size compared to a chilled water store, and 40–48% compared to stores with eutectic salts (Hasnain, 1998).

The developed unit can be used as a freezer and/or a refrigerator, and is suitable for a variety of application such as health, commercial, agricultural and domestic purposes in areas where utility power is unavailable or utility line extensions would be too expensive. In the case where the unit will be used both for refrigerator and freezer, a secondary air-cooled loop can be added in a second compartment. The ability to store ice, instead of electrical energy in batteries, makes the proposed system a multifunction, sustainable and reliable cooling source both day and night without environmental risk.

Compared to kerosene or bottled gas fuelled refrigerators, the proposed system have the advantages of elimination of fuel supply problems, elimination of kerosene fuel and transport costs and finally lower refrigerator maintenance costs. Also, compared to a typical photovoltaic refrigerator/freezer with alternative current compressors, the proposed system has the advantages of elimination of battery, charge controller and inverter inefficiencies and their associated costs.

The aim of this paper is to present the experimental performance evaluation of a certain batteryless ice-making system as well as the experimental behavior of the developed controller which considerably improves startup and steady state operation of photovoltaic powered compressors.

2. System configuration

The ice-making system consists of an insulated ice storage tank filled with water, four small-capacity hermetic compressors equipped with their submerged vertical plate–surface evaporators on which ice is formed, the corresponding air-cooled condensers, a novel controller, and photovoltaic array. The dimensions and configuration of the ice storage tank can permit full immersion of a 25 l milk or water can.

The ice storage tank is an inoxydable tank, has a volume of 175 l and is insulated with polystyrene of 10 cm thickness. Four hermetic type reciprocating, direct-current compressors (Danfoss BD35F-Solar) are used which are connected to a photovoltaic array of 440 W_p, through a controller. The evaporator is an aluminum roll-bond and consists of two plates which have been bonded together over almost their entire surface. The area which is not bonded forms the evaporator channel. It is commercially available, and can readily be defrosted manually. A plate finned tube condenser has been used, and a small-capacity fan forces air between the fins and over the tubes.

Fig. 1 shows the configuration of the system. Four independent cooling compressors are fed through a power controller by a common PV array. The compressors' cooling circuits act on a common water tank. The power ports (P1–P4), the speed ports (C1–C4) of the compressors and the power ports (F1–F4) of the fans are all connected to the system controller.

There is a number of reasons why multiple compressor systems may present advantages over single compressor systems. One advantage is that a much wider control range can be achieved. Even with fixed speed/power compressors, the utilization of energy from a variable power source, like PVs, is increased dramatically when using many small compressors instead of one large compressor (Fig. 2). The same applies to systems with variable speed compressors. For example, a single variable speed compressor can operate at a minimum power of 50% of its rated power. A system of four small, similar compressors, each rated at 1/4 of the single compressor power, will have a total minimum power of operation of 12.5% of the total rated power, since it is possible to operate only one compressor at 50% of its rated power. Another advantage is that the static friction of small compressors is lower than that of large compressors and, as a result, a multiple compressor system has lower startup power requirements. This is of great importance to solar systems, where there is a need for maximum exploitation of the available solar energy. Finally, a multiple compressor system exhibits a much higher degree of

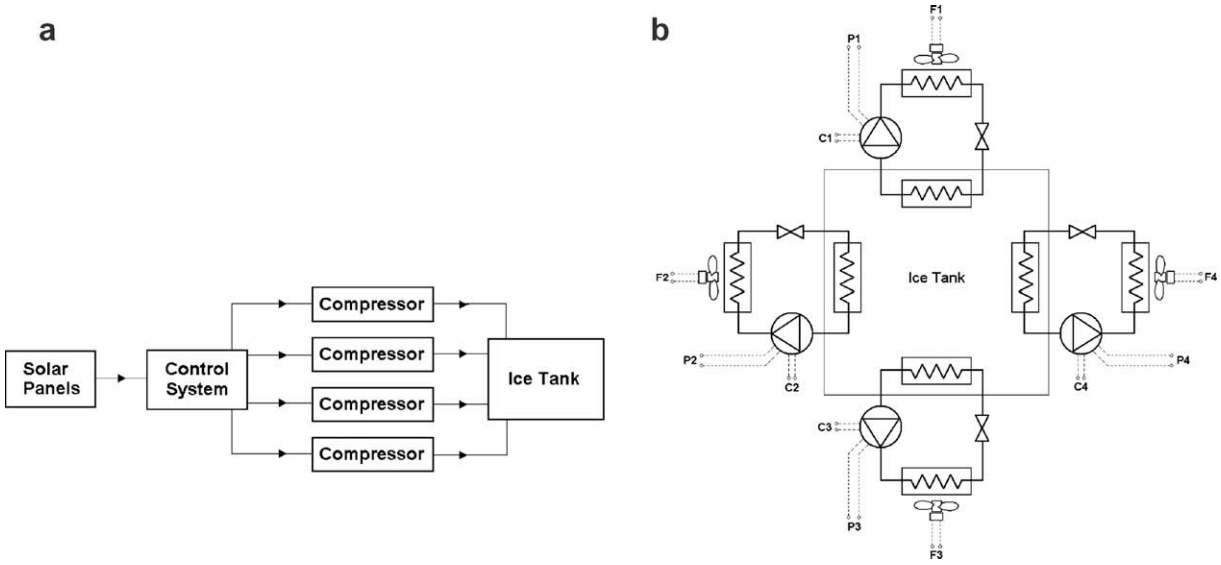

Fig. 1. The ice-maker configuration. (a) Block diagram, (b) The cooling circuits.

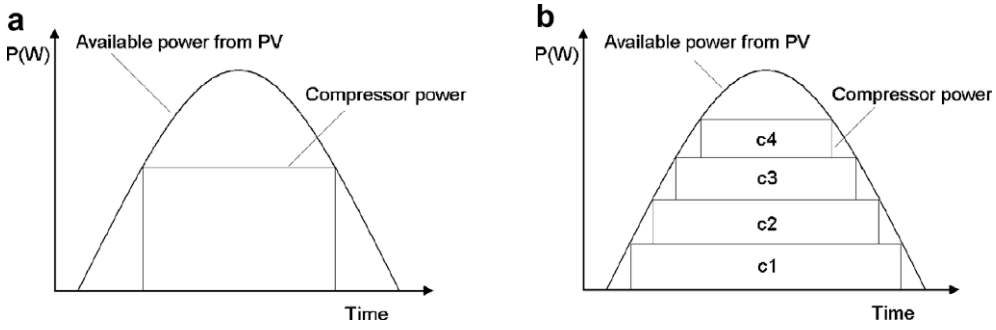

Fig. 2. (a) Operation with single compressor, (b) Operation with multiple compressors.

fault tolerance than a single compressor one since it will sustain the presence of a number of compressor faults before it becomes inoperative.

3. Control system

A dedicated control system has been developed in order to operate the four-compressor arrangement. The control system goals were (a) to alleviate the specific compressors' problematic characteristics, such as the startup and the load management and (b) to operate the four compressors in the most energy-efficient way.

3.1. Startup

As with all motors, the compressor requires a large amount of current at startup in order to overcome its inertia and static friction. The specific compressors might require as much as twice the nominal current at startup, so this requirement of the compressor cannot be satisfied by a PV that provides only the nominal value of compressor current. The result in this case, during startup, is that the effective internal resistance of the PV panel causes a large dip in the panel output voltage. A more macroscopic explanation is that the transient impedance of the compressor is much lower than that of the PV. Fig. 3 depicts the effect. Before startup the compressor is supplied with the PV panel open circuit voltage, point *A*. Right after startup, the compressor causes the drop of the PV output voltage down to point *B*. If the power at that point is sufficient

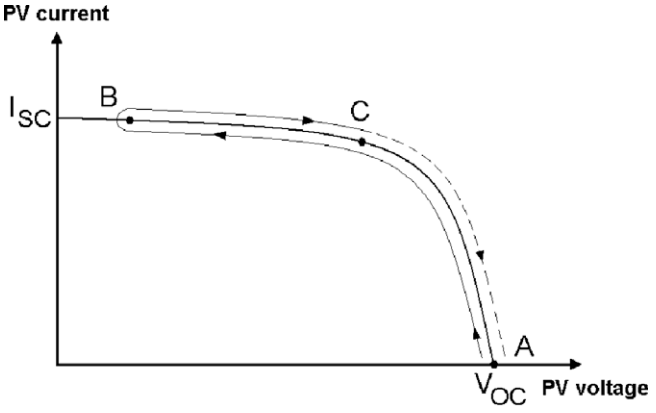

Fig. 3. Compressor start up procedure.

for startup, the compressor will operate normally and its input voltage will slowly rise to a value defined by the current it draws at steady state, point *C*. If the power at point *B* is insufficient for startup, the control circuit will abort the startup procedure and the point of operation in Fig. 3 will return to *A*.

Fig. 4 shows the compressor input voltage (equal to the PV output voltage) waveform from an experiment with a prototype system, a 110 W_p PV panel at a solar irradiance of 420 W/m^2 supplying a BD35F-Solar compressor. Initially, the voltage is around 40 V and during startup it falls down to around 5 V. The PV at the time of the experiment could provide a current of 1 A. Relating this experiment to Fig. 3, one can calculate that the power at point *B* is around 5 W while the PV could provide up to 40 W at point *C*. The power at point *C* is sufficient to start the compressor but the startup transient does not allow the operation at that point. The startup is eventually successful only when the solar irradiance reaches a relatively high level. That is the reason why a solution to the problem is the addition of large capacitors in parallel with the PV. The capacitors 'hold' the PV voltage to a high level while they provide a large transient current to the compressor. Capacitance values of over 50 mF have been used in applications (Pedersen et al., 2004). Such large capacitors increase the cost of the system by a considerable percentage. Another solution is the use of oversized PV panels to provide the startup power at point *B*. This again, is an irrational use of the solar energy and additionally an unjustifiable cost for PV panels.

It would be more efficient if the available PV power at point *C* in Fig. 3 could be used to start the compressor. In order to achieve this, one could design an impedance step-down, Pulse Width Modulated (PWM) converter to ensure that during startup the PV impedance will not be higher than that of the compressor. A converter of this kind is shown in Fig. 5. A switch, *S*, a diode, *D*, and an

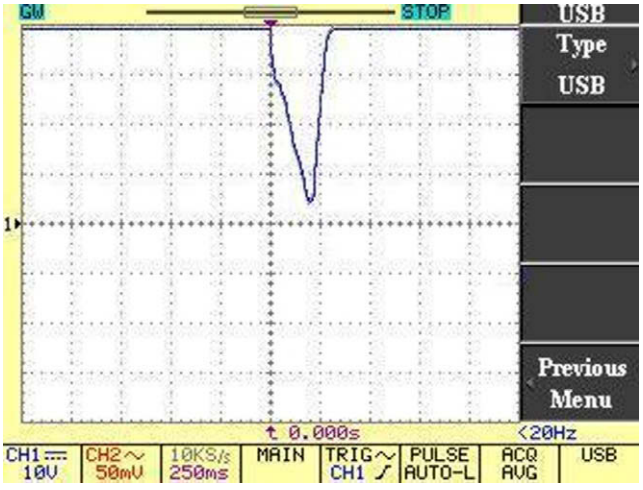

Fig. 4. PV voltage waveform during the compressor startup. Scales: 10 V/div, 250 ms/div.

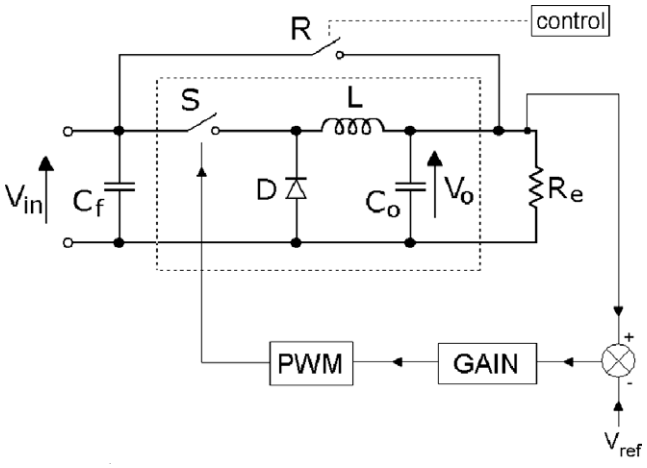

Fig. 5. Impedance converter.

LC filter (L–C_o) form an impedance transformation network, (Mohan et al., 2003), for which it applies that:

$$\frac{V_o}{V_{in}} = D \tag{1}$$

$$\frac{I_o}{I_{in}} = \frac{1}{D} \tag{2}$$

Where V_{in} is the input voltage to the converter (supplied from the PV), V_o is the output voltage of the converter (supplying the compressor) and D is the duty ratio of the switch, which is defined as the *ON* time over the period time, the period being the inverse of the switching frequency. From Eqs. (1) and (2) one can deduce Eq. (3):

$$\frac{Z_o}{Z_{in}} = D^2 \tag{3}$$

Where Z_o and Z_{in} are the output and input impedances of the converter, respectively. Eq. (3) shows that the impedance transformation of the above network can be controlled by the duty ratio of the switch.

The filtering capacitor, C_f, is relatively small, compared to the capacitors used for compressor startup, as it only has to provide high frequency current to the converter. A typical value for it would be less than a couple of milliFarads. The resistance R_e represents the effective internal resistance of the compressors.

The circuit described can be found as a commercial product but unfortunately with fixed frequency response characteristics, a very important point for the required application. One needs to tune the frequency response of the circuit in order to effectively compensate for load transients, these exactly being the startups of the compressor. For the tuning to be performed one needs to know the dynamic transfer function of the compressor or to have the compressor tested. With the circuit of Fig. 5 the optimum startup is achieved on-site by adjusting the gain of the compensating loop with just a few trials.

Since the compressor already includes a converter, the above process could be performed by the compressor itself.

Installing an external converter would introduce extra losses, which is inevitable with all commercial models. However, if one wishes to use an external converter, as was done in this work, these extra losses can be eliminated by employing a smart control procedure. As soon as the compressor starts, the impedance transformation function is no longer needed, so the control circuit can ramp up the duty ratio of the switch up to unity, Fig. 6. The converter inside the compressor will then take control of the impedance transformation needed during steady state (required to accommodate the wide variations in input voltage). Increasing the duty ratio to unity effectively means that the switch of the converter is permanently closed, which brings the switching losses down to zero. Moreover, the conduction losses, due to switch and inductor resistance, can be eliminated by the use of a relay, *R* in Fig. 5, which bridges the input of the converter to the output.

Fig. 7 shows the transient response of the PV-compressor system with the impedance converter connected between the two. This is to be compared to Fig. 4, which was produced under the same conditions. The voltage drop at the input terminals of the compressor is much smaller than that of Fig. 4, and therefore startups are guaranteed at low irradiance levels.

3.2. Load management – maximum power tracking

The speed-power control of the compressor used in this work is normally performed in two modes, either manually or using the manufacturer's control strategy. A variable resistor can be used to control the compressor's speed manually. In manual mode the compressor will operate at constant speed (defined by the control-resistor) and will draw power from the PV depending on the load conditions and not the environmental conditions, i.e. the available PV panel power. For a more efficient operation, the manufacturer of the compressor has incorporated in it an Adaptive

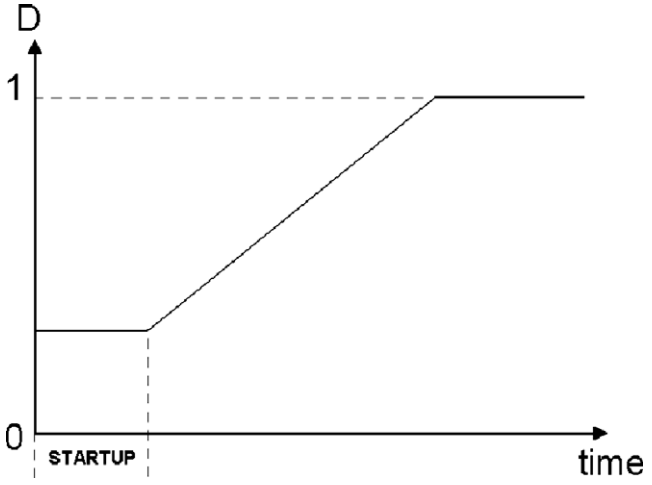

Fig. 6. Duty ratio ramping for minimization of the switching losses.

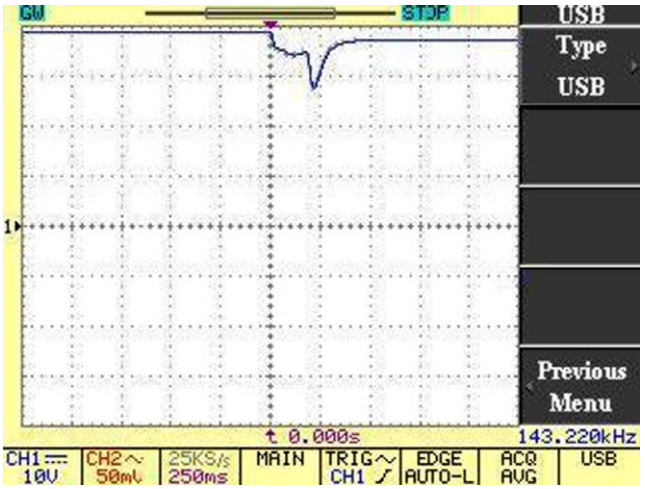

Fig. 7. PV voltage waveform during startup of the compressor with the proposed controller. Scales: 10 V/div, 250 ms/div.

Energy Optimization (AEO) algorithm. In this mode of operation the speed is adjusted to match the capacity needed by the thermal load. However, one can notice from the compressor's datasheet that, even though sufficient energy may be available, the compressor, in the AEO mode, will not reach maximum speed directly but with a speed increase rate of 12.5 rpm/min. This characteristic causes a considerable energy loss when the compressor is operated on days with wide solar irradiance variations. Fig. 8 shows the result of a comparative experiment carried out with two identical compressors operating in different mode; one in the aforementioned manufacturer supplied AEO mode of operation and the other in our developed maximum power tracking (MPT) mode of operation to be discussed. The compressor is connected to a cooling circuit and is left to operate from a PV panel for the duration of a day with wide irradiance variations. It is noticeable that the compressor power, in AEO mode, lags the varia-

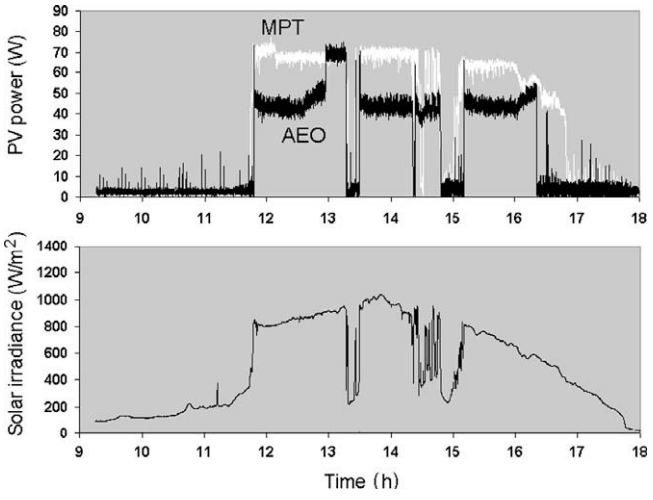

Fig. 8. Variation of solar irradiance, and PV power in two modes (AEO, MPT).

tions in irradiance and does not reach maximum power, for each specific irradiance level, directly but after about 40 min of operation. This energy loss is enlarged by the fact that the compressor stops at several time points due to low irradiance.

A maximum power tracking (MPT) control system can be used, in conjunction with a speed-control input on the compressor, to extract the maximum electric power from the PV at any time. The control method presented below is simple enough to be implemented by the compressor's internal microprocessor.

For a fixed load, the output current and voltage of the PV can be measured once and the PV equivalent internal impedance can be calculated. An impedance converter can then supply the load in a way that it emulates the internal source impedance and therefore MPT is achieved. However the PV internal impedance is not fixed under all conditions. Extra, on-line measurements are required if a variable load and/or internal impedance are considered, which is the case here. In an attempt to reduce the number of sensors, fuzzy logic systems and Perturb And Observe methods may be employed, (Hong and Hamill, 2000; Sugimoto and Dong, 1997; Wolf and Enslin, 1993; Senjyu and Uezato, 1994; Veerachary et al., 2002; Tse et al., 2002), which require only the PV voltage and current measurement. The control system injects a disturbance in a converter, which supplies the load, and detects the derivative of the PV power. It then operates the converter in a way that forces the derivative to zero and therefore maximum power tracking is achieved, irrespective of the loading or source conditions. A similar system was used in this work but without the employment of an additional converter. The converter already described is only responsible for the startup of the compressor and is expected to be replaced by the converter inside the compressor. The speed-control input of the compressor was used for MPT. Fig. 9 shows the block diagram of the process. The voltage and current of the PV are sampled and the drawn power is measured by a computer. The computer injects perturbations to the compressor by means of its speed-control input (a resistor-controlled input). Changing the speed-control resistance (with a 4-bit system) results in a change in compressor speed, which ultimately results in a perturbation in the current drawn by the compressor (Fig. 10). Using a special algorithm the computer manages to force the operating point of the compressor around the maximum power point of the PV.

The performance of the controller is shown in Fig. 8. The MPT control system forces the compressor power to follow the available PV panel energy, indicated by the irradiance level, and therefore achieves much higher energy utilization than that with the AEO mode. The MPT algorithm is relatively simple and does not require high computational power. It can therefore be embedded in the PIC microcontroller already installed in the BD35F compressor. Similarly, the impedance conversion can be implemented by the compressor's internal converter. The proposed solution is thus fairly practical while it can result in impressive increase of the system performance.

3.3. Multiple compressor operation

The power drawn by each compressor is roughly proportional to its speed. Therefore, in order to adapt the compressors to the solar panel one needs to modify the compressors' speed according to the available power. For a single compressor this function can be performed through the maximum power tracking control mentioned above. However, when multiple compressors are operated at the same time, one needs to consider a suitable pattern of operation, in conjunction with maximum power tracking.

Fig. 11 shows the proposed compressors control pattern. At low PV power levels only one compressor can be started and operated. As the power level increases the compressor's speed is increased automatically by the maximum power tracking control. At some point in time the compressor reaches its maximum speed. In order to start a second compressor one would have to wait until the PV panel provided another 50–60 W, which are required for the second

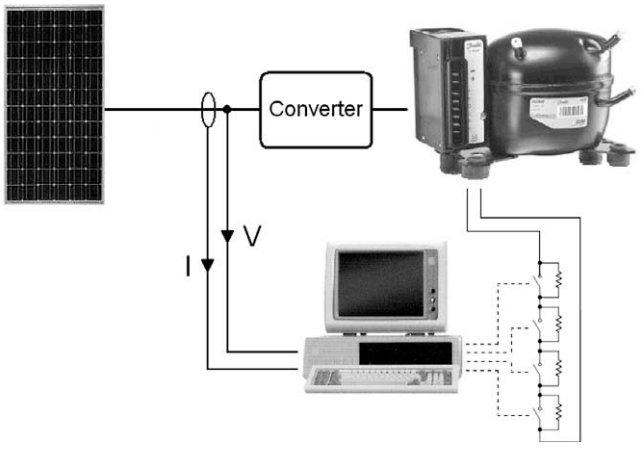

Fig. 9. Maximum power tracking arrangement.

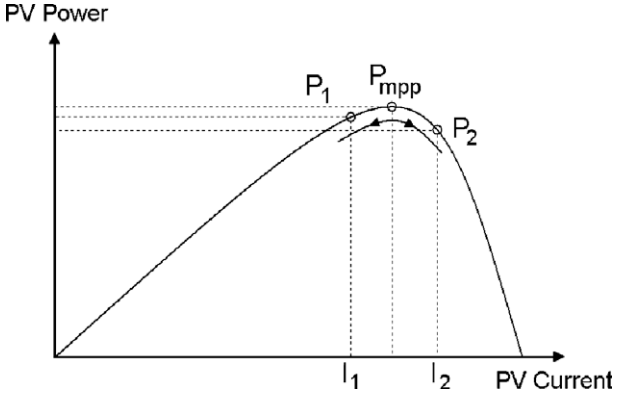

Fig. 10. Perturbations on the power curve of a PV, showing the maximum power point (mpp).

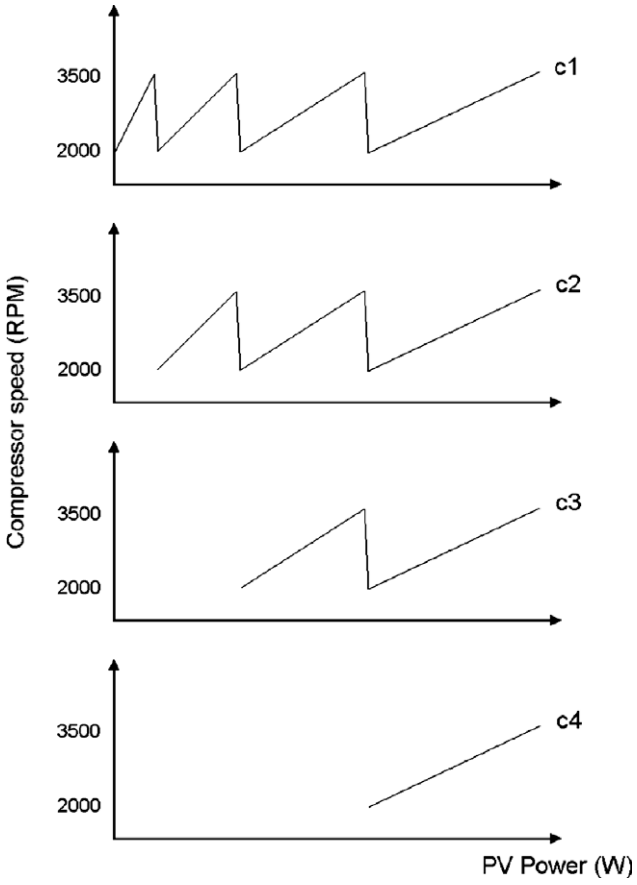

Fig. 11. Speed control pattern for the four compressors (c1–c4).

compressor startup. In the mean time the first compressor would not be capable of utilizing the extra energy since it is driven at maximum speed, which means that there would be underutilization of the PV generated energy. If, for instance, the first compressor reached maximum speed and then the PV supplied an excess power of only 40 W (lower than needed to start the second compressor) for 1 h (due to environmental conditions) there would be 40 Whrs unused. It is therefore proposed here that the first compressor speed should fall to minimum (right after it reaches maximum speed) in order to leave an available power level for the second compressor to start. In this way the second compressor can start immediately after the first one reaches maximum power (Fig. 11). If excess power is available, both compressors will speed up to their maximum speed and the previous procedure will be repeated for the rest two compressors. Fig. 11 shows that the speed-up rate (with regard to power increase) decreases as more compressors become active.

The above-described operation is more efficient not only due to better energy utilization but also due to the characteristics of the compressors. The compressors are characterized by a higher value of Coefficient Of Performance (COP) at low speeds. Fig. 12, shows the variation of this coefficient with speed for a given evaporation temperature, according to the company's specifications for the used compressor (Danfoss, 2003). Since this temperature remains roughly constant throughout the formation of the ice, it is desirable to have all compressors driven at the same speed rather than having some at their maximum speed and modifying the speed of the last one according to the available power.

The effectiveness of the presented speed control method will be shown in the results section.

4. Instrumentation

In order to evaluate the performance of ice-making system, a PC-based automatic data acquisition unit has been used. The unit monitors total solar irradiance on the tilted PV modules' surface, array voltage and current, ambient temperature, cell temperature, low and high pressure across the compressor, inlet and outlet temperature of the refrigerant at the compressor, and temperature at different points in the water tank. The unit scanned all channels in ten seconds intervals, averaged them over 1 min periods and stored them in a hard disk for further processing. The solar irradiance was measured using a first class pyranometer. Current, voltage and pressure were measured by relevant sensors, and finally all temperatures were measured with platinum resistance detectors.

The system operated daily and the ice produced was weighed at the end of the day. At the beginning of each day, before the start of the test, the system was preconditioned so as to have the system always starting with the same condition. The condition was that there was no ice formed on the cooling plates and that the water was at the ice nucleation temperature that is the temperature at which ice begins to form. From this point the ice is formed and it grows as dendritic ice, which consists of thin plate-like crystals of ice interspersed in the water (Akyurt et al., 2002). This condition was dictated by the practical use of the ice-maker in which the system would start operating every day having kept a fair amount of ice from the previous day. That amount of ice would keep the water

COP (EN 12900 Household/CECOMAF)

rpm \ °C	-30	-25	-23.3	-20	-15	-10	-5	0	5	7.2	10	15
2,000	0.90	1.02	1.06	1.15	1.31	1.48	1.67	1.87	2.08	2.17	2.29	
2,500	0.87	0.97	1.01	1.09	1.24	1.41	1.60	1.80	2.02	2.12		
3,000	0.75	0.90	0.95	1.06	1.22	1.39	1.58	1.78				
3,500	0.73	0.84	0.89	1.00	1.17	1.36	1.55					

Fig. 12. Coefficient Of Performance (COP) variation with speed for a given evaporation temperature.

temperature at around 0 °C at all times. The ice is removed from the plates at the end of the day in order to measure the exact amount of ice produced during the day.

5. Results and discussion

Several experimental measurements were taken throughout many months and the collected data was used to evaluate the behavior of the proposed controller and the energy efficiency and ice-making capability of the system.

Fig. 13 shows the PV power of the ice-maker and the solar irradiance during a sunny day (17-11-2006). The first compressor starts operating at around 8:30, quite early for a November day. The startup is significantly aided by the dedicated startup converter described above. A single high power compressor without a startup system would have required a solar irradiance of at least 400 W/m^2 in order to perform a startup, while the proposed system started at 150 W/m^2. Right after startup the compressor enters the maximum power tracking mode. It is visible that there is a coincidence of the supplied PV power and the solar irradiance curves. Since the available PV power is almost proportional to the solar irradiance one may directly reach to the conclusion that all the available PV power is being drawn from the PVs and delivered to the compressor. After a small period of time the second compressor is started. This is visible as a short/sharp reduction in power at around 9:00. That is where the controller decides to lower the speed/power of the first compressor to minimum so as to gain a power margin for the startup of the second compressor. Again, right after the startup of the second compressor, the two compressors enter the maximum power tracking mode and precisely follow the available PV power. The same is done with the rest two compressors. Between 12:00 and 14:00 the system does not exceed a maximum power, which corresponds to the total rated power of the compressors. The PVs are slightly oversized, which fact gives an advantage in early startup and in the operation on cloudy days. The same operation pattern is followed during the descent of the solar irradiance.

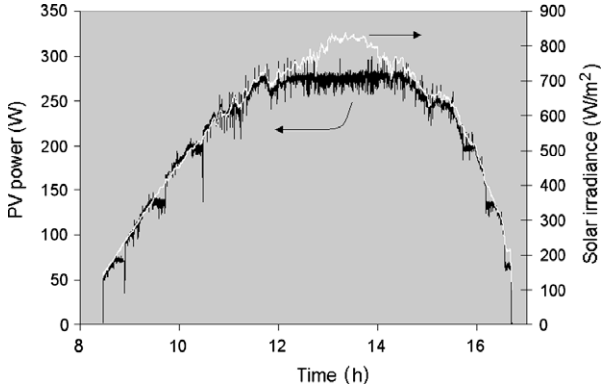

Fig. 13. Variation of PV power and solar irradiance on a sunny day.

Fig. 14 shows the operation of the ice-maker on a day with wide irradiance variations (28-3-07). The system manages again to precisely follow the variations of the solar irradiance and effectively utilises all the available energy, despite the fact that the solar irradiance profile is fairly abnormal and contains sharp edges of great amplitude. Fig. 15 shows a closer look at the 9:00–10:00 interval in order to reveal the response of the decision-making algorithm. It is evident that the number of operating compressors is chosen quite fast, according to the level of the solar irradiance. The level of activation for the compressors has been found experimentally and certain margins have been allowed so as to ensure successful startups. The above response of the control system enables the ice-maker to operate with any irradiance profile.

The complete ice-maker was tested on days with different values of total solar irradiation in order to evaluate the amount of produced ice. Fig. 16 shows the performance curves of the ice-maker as regards the daily solar irradiation on the tilted surface of the PV array. The compressor

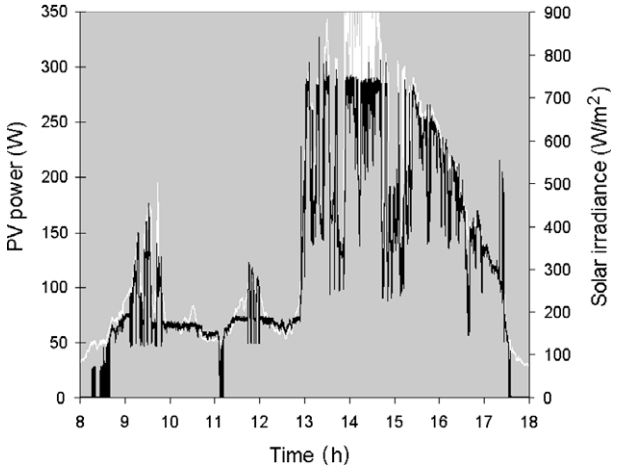

Fig. 14. Variation of PV power and solar irradiance on a day with wide irradiance variations.

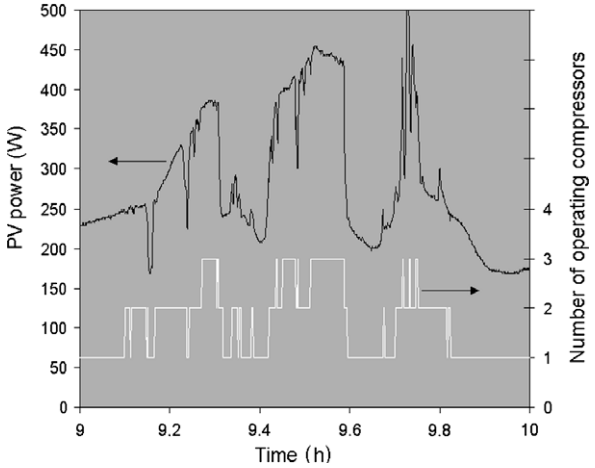

Fig. 15. Response of the decision-making algorithm.

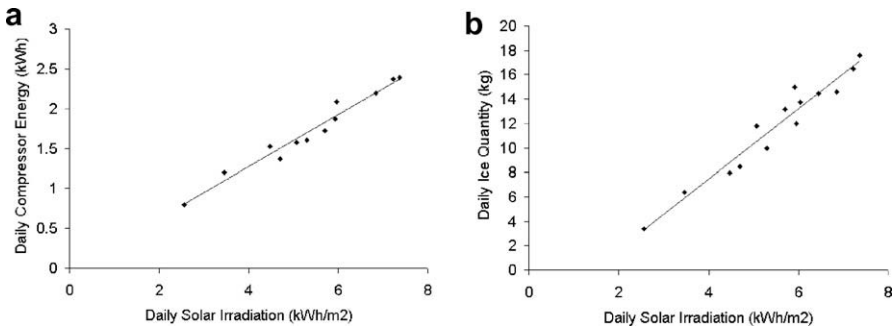

Fig. 16. The performance curves of the ice-maker. (a) Energy exploitation, (b) Ice formation.

energy exploitation curve (a), can be approximated by a linear function with a proportionality constant of around 0.303 kWh(compressor)/kWh/m^2, which, taking into account the PV area of 3.3 m^2, suggests a combined PV panel – compressor efficiency of around 9.2%. This value is quite close to the PV panel nominal efficiency, revealing the accurate maximum power tracking of the controller.

The ice quantity curve, Fig. 16(b), shows that the system is capable of producing around 4.5 kg of ice at only 3 kWh/m^2 and up to 17 kg at about 7.3 kWh/m^2, all units per day. One may notice large deviations in the values in this graph. These deviations are largely due to the impact of the solar irradiance profile on the system performance. Two days with the same total solar irradiation but different solar irradiance profile may lead to the production of different quantities of ice. This effect can be attributed to the Coefficient Of Performance of the compressors in combination with the compressors' speed at different solar irradiance levels. Also, the ambient temperature can affect the performance of the PV array and the condensers and the thermal losses of the ice storage tank, therefore affecting the daily ice production.

6. Conclusions

A batteryless, solar-powered ice-maker has been presented that is truly autonomous and environmentally friendly. The ice energy storage renders the systems maintenance-free and makes it ideal for application in remote areas with energy supply limitations. The system controller offers a reliable operation with near-perfect solar energy utilization, making the solar-to-compressor power efficiency reach around 9.2%. This is done by providing easy compressor startups, enabling operation at as low as 150 W/m^2 of solar irradiance, accurate maximum power tracking and efficient power management. The prototype results have shown that the system energy exploitation is very high and that the system can produce a relatively large quantity of ice (up to 17 kg from a 440 W_p PV panel on a good day), even on days with low total solar irradiation. These results verify the success of the proposed ice-maker configuration in providing a reliable continuous cooling source for a wide range of solar irradiance levels.

Acknowledgements

This work was co-funded by 75% from the European Union and 25% from the Greek Government under the framework of the Education and Initial Vocational Training Program – Archimedes.

References

Akyurt, M., Zaki, G., Habeebullah, B., 2002. Freezing phenomena in ice-water systems. Energy conversion and management 43, 1773–1789.

Bessler, W.F., Hwang, B.C., 1980. Solar assisted heat pumps for residential use. ASHRAE Journal 59, 63.

Boubakri, A., 2006. Performance of an adsorptive solar ice maker operating with a single double function heat exchanger (evaporator/condenser). Renewable Energy 31, 1799–1812.

Buchter, F., Dind, Ph., Pons, M., 2003. An experimental solar-powered adsorptive refrigerator tested in Burkina-Faso. International Journal of Refrigeration 26, 79–86.

Chatuverdi, S.K., Abazeri, M., 1987. Transient simulation of a capacity-modulated, direct-expansion solar-assisted heat pump. Solar Energy 39, 1421–1428.

Chatuverdi, S.K., Chen, D.T., Kheireddine, A., 1998. Thermal performance of a variable capacity direct expansion solar-assisted heat pump. Energy Conversion and management 39, 181–191.

Danfoss, 2003. www.danfoss.com.

Diaz, P., Lorenzo, E., 2001. Solar Home System battery and charge regulator testing. Progress in Photovoltaics: Research and Applications 9, 363–377.

El Tom, O.M.M., Omer, S.A., Taha, A.Z., Sayigh, A.A.M., 1991. Performance of a photovoltaic solar refrigerator in tropical climate conditions. Renewable Energy 1, 199–205.

Hasnain, S.M., 1998. Review on sustainable thermal energy storage technologies. Part II: cool thermal storage. Energy conversion and management 39, 1139–1155.

Hawlader, M.N.A., Chou, S.K., Ullach, M.Z., 2001. The performance of a solar assisted heat pump water heating system. Applied Thermal Engineering 21, 1049–1065.

Hildbrand, C., Dind, P., Pons, M., Buchter, F., 2004. A new solar powered adsorption refrigerator with high performance. Solar Energy 77, 311–318.

Hong, L.Y., Hamill, D.C., 2000. Simple maximum power point tracker for photovoltaic arrays. Electronics Letters 36, 997–999.

Kaplanis, S., Papanastasiou, S., 2006. The study and performance of a modified conventional refrigerator to serve as a PV powered one. Renewable Energy 31, 771–780.

Kattakayam, T.A., Srinivasan, K., 1998. Uninterrupted power supply for autonomous small refrigerators. Energy Conversion and Management 39, 21–26.

Kattakayam, T.A., Srinivasan, K., 2000. Thermal performance characterization of a photovoltaic driven domestic refrigerator. International Journal of Refrigeration 23, 190–196.

Khattab, N.M., 2006. Simulation and optimization of a novel solar-powered adsorption refrigeration module. Solar Energy 80, 823–833.

Kuang, Y.H., Sumathy, K., Wang, R.Z., 2003. Study on a direct-expansion solar-assisted heat pump water heating system. International Journal of Energy Research 27, 531–548.

Leite, A.P.F., Daguenet, M., 2000. Performance of a new solid adsorption ice maker with solar energy regeneration. Energy Conversion and Management 41, 1625–1647.

Li, M., Huang, H.B., Wang, R.Z., Wang, L.L., Cai, W.D., Yang, W.M., 2004. Experimental study on adsorbent of activated carbon with refrigerant of methanol and ethanol for solar ice maker. Renewable Energy 29, 2235–2244.

Li, Y.W., Wang, R.Z., Wu, J.Y., Xu, Y.X., 2007. Experimental performance analysis and optimization of a direct expansion solar-assisted heat pump water heater. Energy 32, 1361–1374.

Luo, H.L., Dai, Y.J., Wang, R.Z., Tang, R., Li, M., 2005. Year round test of a solar adsorption ice maker in Kunming, China. Energy Conversion and Management 46, 2032–2041.

Mohan, N., Undeland, T.M., Robbins, W.P., 2003. Power electronics—Converters. In: Applications and Design. Hoboken, John Wiley & Sons Inc., New Jersey.

Pedersen, P. H., Poulsen, S., Katic, I., 2004. Solarchill – a Solar PV Refrigerator without Battery. In: EuroSun 2004 Conference, Freiburg, Germany.

Senjyu,T., Uezato, K., 1994.Maximum power point tracker using fuzzy control for photovoltaic arrays. In: Proceedings of the IEEE International Conference on Industrial Technology, Guangzhou. China, pp. 143–147.

Spiers, D.J., Rasinkoski, A.A., 1996. Limits to battery lifetime in photovoltaic applications. Solar Energy 58, 147–154.

Stevens, J., Kratochvil, J., Harrington, St., 1993. Field investigation of the relationship between battery size and PV system performance. In: Proceedings of 23rd IEEE PV Specialists Conference, Louisville, pp. 1163–1169.

Sugimoto, H., Dong, H., 1997. A new scheme for maximum photovoltaic power tracking control. In: Proceedings of the Nagaoka Power Conversion Conference, Nagaoga, Japan, vol. 2, pp. 691–696.

Taha, A.Z., 1995. The oversizing method of estimation in PV systems. Renewable Energy 6, 487–490.

Toure, S., Fassinou, W.F., 1999. Cold storage and autonomy in a three compartments photovoltaic solar refrigerator: experimental and thermodynamic study. Renewable Energy 17, 587–602.

Tse, K.K., Ho, M.T., Chung, H.S.-H., Hui, S.Y., 2002. A novel maximum power point tracker for PV panels using switching frequency modulation. IEEE Transactions on Power Electronics 17, 980–989.

Veerachary, M., Senjyu, T., Uezato, K., 2002. maximum power point tracking control of PV system. IEEE Transactions on Aerospace and Electronic Systems 38, 262–270.

Wagner, R., Sauer, D.U., 2001. Charge strategies for valve-regulated lead/acid batteries in solar power applications. Journal of Power Sources 95, 141–152.

Wang, R.Z., Li, M., Xu, Y.X., Wu, J.Y., 2000. An energy efficient hybrid system of solar-powered water heater and adsorption ice maker. Solar Energy 68, 189–195.

Wolf, S.S.M., Enslin, J.H.R., 1993. Economical, PV maximum power point tracking regulator with simplistic controller. In: Proceedings of the 24th Annual IEEE Power Electronics Specialists Conference, pp. 581–587.

Woodworth, J., Thomas, M., Stevens, J., Harrington, S., Dunlop, J., Ramu Swany M., Demetrius, L., 1994. Evaluation of batteries and charge controllers in small stand-alone PV systems. In: Proceedings of the 24th IEEE Photovoltaic Specialists Conference, Hawaii, pp. 933–945.